

Detection of NH Stretching Signals from the Monolayers of Amino Acid Amphiphiles at the Air–Water Interface and Change of Hydrogen Bond Depending on Metal Ion in the Subphase: Infrared Reflection–Adsorption Spectroscopy

Xuezhong Du* and Yingqiu Liang*

Key Laboratory of Mesoscopic Chemistry, Ministry of Education, Department of Chemistry, Nanjing University, Nanjing 210093, People's Republic of China

Received: November 18, 2003; In Final Form: February 26, 2004

The monolayers of amino acid amphiphiles at the air–water interface on pure water and ion-containing subphases have been studied using infrared reflection–absorption spectroscopy. It is the first time that the NH stretching signals are detected from the monolayers at the air–water interface with this technique. In the presence of Ag^+ and Pb^{2+} in the subphases, the covalent interaction between metals and carboxylate groups is predominant in the form of chelating and/or bridging bidentate coordination, and the intermolecular hydrogen-bonding interaction between the adjacent molecules through amide groups is increased in comparison with that in the case of pure water. In the presence of Ca^{2+} and Cu^{2+} , the ionic interaction between metal ions and carboxylate groups is preferred, and the intramolecular hydrogen bond is developed. The hydrogen bond in the monolayers at the air–water interface undergoes an obvious change in type and strength depending on metal ion in the subphase.

Introduction

Chirality is a very important phenomenon in nature. Chirality in proteins is observed to originate from geometrical as well as topological features.¹ Geometrical chiral features observed in proteins are the asymmetrically substituted tetrahedral carbon atom of L-amino acids, twisted peptide chains, helices, cylindrical packing of helices, etc.² The studies of chirality-dependent intermolecular forces in two-dimensional self-assemblies are of tremendous importance in many biological processes. Nandi and Vollhardt² recently reviewed effect of molecular chirality on the morphology of biomimetic Langmuir monolayers on the basis of the experimental results obtained mainly from surface pressure (π)–area (A) isotherm, Brewster angle microscopy (BAM), fluorescence microscopy, and grazing incidence X-ray diffraction (GIXD). Thermodynamic measurements such as π – A isotherms do not reveal significant chiral discrimination effects in many cases. BAM and fluorescence microscopy can directly visualize the morphologies of the monolayers composed of chiral molecules; however, these observations are confined to macroscopic and mesoscopic scales^{3,4} and can determine neither molecular characteristics such as conformation and packing of the alkyl chains nor structure and interaction pattern of the headgroups. Although the GIXD technique is a valuable tool to obtain direct structural information of crystalline films at the interfaces at the subnanometer scale,⁵ infrared reflection–absorption spectroscopy (IRRAS) has emerged as one of the leading structural analyses for monolayers at the air–water interface over the past decade^{6–19} since the early works by Dluhy and co-workers.^{20–22} The IRRAS technique not only allows for the characterization of chain conformation/orientation and headgroup structure but also provides valuable information about molecular interaction between the monolayers and substances dissolved in the subphase. Hühnerfuss and co-workers^{7–9} studied

in detail the correlation between the chiral discrimination effect and the chain order/headgroup structure of *N*-acyl amino acid monolayers at the air–water interface using this technique with unpolarized radiation, but some valuable information on the molecular structure and interaction fashion is limited due to the relatively weak signals and the disturbance of water vapor. On the other hand, the structure of water adjacent to the monolayers is altered due to the interactions with the headgroups of the film constituents. The baseline distortion due to the water absorption is significant in the case of optimal incidence angles such as 30°.

Hydrogen bond has crucial importance in many chemistry research areas. The NH stretching mode is usually used as a fingerprint of the hydrogen bond for structural analysis and molecular recognition. The formation of hydrogen-bonding networks between complementary components has been investigated at the air–water interface using IRRAS technique.^{10,15,16,23} To the best of our knowledge, the vibrational bands above 3000 cm^{-1} except water absorption bands have not so far been reported, e.g., NH stretching mode, for the monolayers at the air–water interface. In this paper, the NH stretching bands are distinctly observed from *N*-octadecanoyl-L-alanine monolayers at the air–water interface using the IRRAS technique, and the hydrogen bond existed in the monolayers undergoes an obvious change in type and strength in the presence of metal ions in the subphase.

Experimental Section

Materials. The synthesis of *N*-octadecanoyl-L-alanine sample was reported in detail.²⁴ The chemical reagents used were of analytical grade and the water used was double distilled after a deionized Milli-Q exchange. The pH value of pure water was adjusted to 3.0 by the addition of HCl, but the pH values of the ion-containing subphases (1 mM, Ag^+ , Pb^{2+} , Ca^{2+} , and Cu^{2+}) were their self-buffered values without the addition of HCl or NaOH.

* To whom correspondence should be addressed. E-mail: duxz2000@yahoo.com (X.D.); yqliang@nju.edu.cn (Y.L.). Fax: 0086–25–3317761.

IRRAS Spectral Measurements. IRRAS measurements of *N*-octadecanoyl-L-alanine monolayers at the air–water interface were performed on an Equinox 55 FT-IR spectrometer equipped with a Bruker XA-511 external reflection attachment with a shuttle Langmuir trough using a mercury–cadmium–telluride (MCT) detector. The surface pressures were always monitored during IRRAS scans. The temperature was set to 22 °C. The spectra were recorded with a resolution of 8 cm⁻¹ by coaddition of 2048 scans unless otherwise stated, and a relatively high signal-to-noise ratio could be obtained by carefully controlling the experimental conditions. The external reflection–absorption spectra of pure water (pH 3.0) and 1 mM ion-containing solutions were used as references, respectively. All of infrared spectra were used without any smoothing. The film-forming molecules were spread from chloroform solutions of desired volumes. After the chloroform was evaporated, the measurement system was enclosed for the equilibrium of humidity and the relaxation of the monolayers for 4 h prior to compression. The monolayers were then compressed discontinuously to surface pressures at the set values. Twenty minutes were allowed for the relaxation of the films before spectral measurement. In the scanning procedures, the surface pressures were held at the target pressures by adjusting the moving barriers forward or backward slightly. There are two advantages for the use of a shuttle system in the experimental setup:¹⁷ one is a good water vapor match between reference and sample, and the other is the spectra of s- and p-polarized radiation could be acquired from the same monolayer by switching the KRS-5 polarizer to s or p polarization. Polarizer efficiency was reported to be about 99.2% for the same accessory.¹²

Monolayer Transfer and FTIR Spectral Measurements. The monolayer spreading and transfer were performed on a homemade Langmuir trough equipped with computer controls. A paper Wilhelmy plate was used as the surface pressure sensor and hung in the middle of the trough. Two barriers compressed or expanded symmetrically at the same rate from two sides of the trough. After spreading, twenty minutes was allowed for solvent evaporation. Eleven-monolayer Langmuir–Blodgett (LB) films were deposited onto CaF₂ substrates by the vertical method (dipping rate 2 mm/min) at the surface pressures of 20 and 30 mN/m with a transfer ratio of 0.9–1.0 at room temperature, respectively. For the LB film prepared near 0 mN/m, the monolayer was first compressed up to the surface pressure about 0.1 mN/m, the first monolayer was transferred onto a CaF₂ substrate with the vertical method to obtain a hydrophobic surface, and the following monolayers were transferred by the horizontal lifting with a transfer ratio of about 2.0. FTIR transmission spectra were recorded on a Bruker IFS 66V spectrometer equipped with a deuterated triglycine sulfate (DTGS) detector. Typically, 1000 interferograms were collected to obtain a satisfactory signal-to-noise ratio with a resolution of 4 cm⁻¹.

Results and Discussion

Detection of NH Stretching Signals from the Monolayers.

Figure 1 shows the IRRAS spectra of *N*-octadecanoyl-L-alanine monolayers on acidified water (pH 3.0) at various surface pressures. All of the negative reflection–absorption bands increase in intensity with surface pressure, and their frequencies at the lower surface pressures are nearly the same as those at 20 mN/m except for the bands near 1730–1705 cm⁻¹ due to the C=O stretching vibration of carboxylic acid. The two bands at 2919 and 2851 cm⁻¹ are assigned to the asymmetric and symmetric CH₂ stretching modes [$\nu_a(\text{CH}_2)$ and $\nu_s(\text{CH}_2)$],

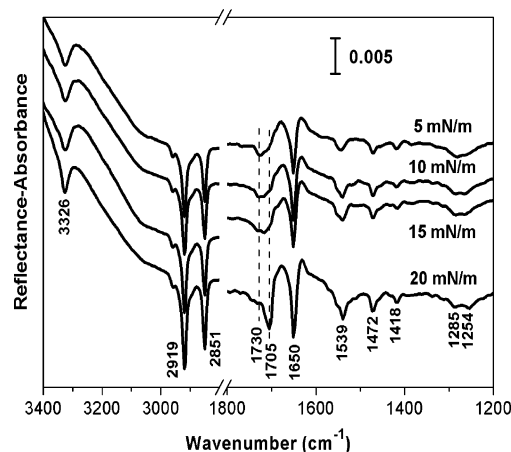


Figure 1. IRRAS spectra of the monolayers of *N*-octadecanoyl-L-alanine on acidified water (pH 3.0) at various surface pressures: radiation, p polarization; incidence angle, 30°; temperature, 22 °C.

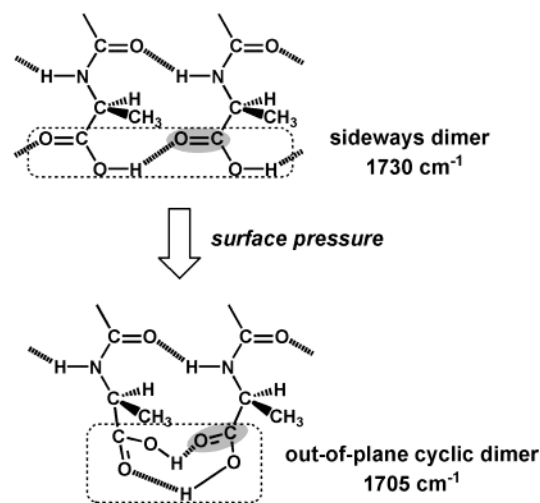


Figure 2. Schematic illustration of formation of intermolecular hydrogen bond and change of carboxylic acid dimers.

respectively, which indicates that the alkyl chains predominantly take an ordered conformation.²⁵ The singlet peak at 1472 cm⁻¹ due to the CH₂ scissoring mode [$\delta(\text{CH}_2)$] indicates that the alkyl chains in the monolayers are in a triclinic crystal form where adjacent C–C–C planes are packed in a parallel fashion.²⁶ Although the spectral resolution 8 cm⁻¹ is used for the collection of the IRRAS spectra, it is unlikely that a doublet for the $\delta(\text{CH}_2)$ mode appears due to an orthorhombic subcell structure. This is because the herringbone arrangement generated glide symmetry prevents the formation of favorable intermolecular N–H...O=C bonds² between adjacent amide groups as shown in the following. A weak peak around 1418 cm⁻¹ is assigned to the bending mode of the CH₂ groups adjacent to the amide groups [$\delta(\text{C}_\alpha\text{H}_2)$]. The 1705 cm⁻¹ component due to the C=O stretching vibration of the carboxylic acid increases gradually at the expense of the 1730 cm⁻¹ one with surface pressure. The 1730 and 1705 cm⁻¹ components are associated with the sideways dimers^{27,28} and out-of-plane cyclic dimers²⁴ of carboxylic acid groups (see Figure 2), respectively.

The bands at 3326, 1650, and 1539 cm⁻¹ in Figure 1 are assigned to amide A [$\nu(\text{NH})$], amide I [$\nu(\text{C}=\text{O})$], and amide II [$\delta(\text{NH})$] bands,²⁴ respectively. The $\nu(\text{NH})$ bands are for the first time clearly observed in the IRRAS spectra of the monolayers at the air–water interface, even at the lower surface pressures. The position and shape of the $\nu(\text{NH})$ bands can provide information on type and strength of hydrogen bond, which will

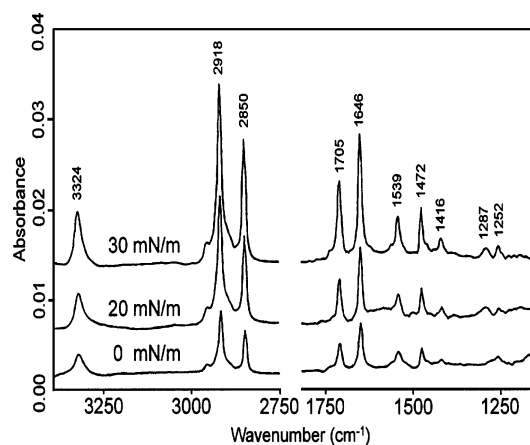


Figure 3. FTIR transmission spectra of 11-monolayer *N*-octadecanoyl-L-alanine LB films transferred from pure water (pH 3.0) at various surface pressures.

give a deep insight into elucidating the interactions not only between adjacent molecules in the monolayers but also between the headgroups and substances in the subphase. In the case of unassociated states, the amide A band appears around 3450 cm^{-1} , and the amide II band at 1510 cm^{-1} .²⁹ Generally, the $\nu(\text{NH})$ frequency lower than 3350 cm^{-1} indicates that the amide groups are engaged in hydrogen-bonding interaction. The amide A and amide II bands in Figure 1 take a shift to lower and higher frequencies, respectively, in comparison with those in the unassociated states,²⁹ which suggests the occurrence of hydrogen-bonding interaction between the adjacent molecules through the amide groups (see Figure 2). The FTIR transmission spectra of the corresponding LB films at various surface pressures are shown in Figure 3 for comparison. In the case of LB films free of water, the amide A bands are located at 3324 cm^{-1} , which are very similar to the bands at 3326 cm^{-1} in Figure 1. This provides confirmative evidence for the NH stretching band observation from the monolayers at the air–water interface. The probable reasons that the NH stretching signals can be detected in our case are speculated in the following: (1) the signal intensity is related to the property of amide groups (e.g., the NH stretching signals from amide are, typically, stronger than those from amine); (2) the shuttle system is used to diminish the disturbance of water vapor so that the reflection–absorption signals in the range can be discernible, but it is not a sufficient condition for the observation. In our recent paper,²³ no NH stretching signal was clearly observed from the IRRAS spectra of 1-(2-((octadecyloxy)carbonyl)ethyl)cytosine monolayers at the air–water interface as obtained from the FTIR transmission spectra of the corresponding LB films;³⁰ (3) the intermolecular hydrogen-bonded network between the amide groups prevents them from contacting with subphase water and suppresses the interaction with water molecules. One obvious difference between Figures 1 and 3 is that only the 1705 cm^{-1} component of the carboxylic acids in the LB films is observed, even at about 0 mN/m . The $\nu(\text{C}=\text{O})$ band at 1705 cm^{-1} indicates that the carboxylic acid cyclic dimers are formed between neighboring monolayers in the LB films.

Change of Hydrogen Bond Depending on Metal Ion.

Figure 4 shows the IRRAS spectra of *N*-octadecanoyl-L-alanine monolayers on pure water (pH 3.0) and ion-containing subphases. The original $\nu(\text{C}=\text{O})$ band at 1705 cm^{-1} observed on the pure water surface completely disappears on the ion-containing subphases. Some new bands appear in the region $1600\text{--}1500\text{ cm}^{-1}$ and are attributed to the asymmetric stretching of carboxylate groups. Ag^+ and Pb^{2+} ions lead to the formation

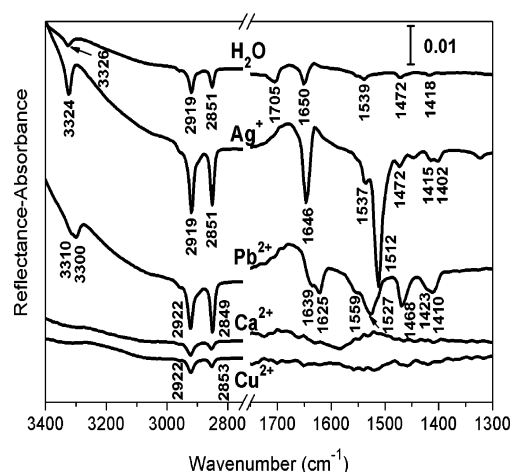


Figure 4. IRRAS spectra of the monolayers of *N*-octadecanoyl-L-alanine on ion-containing subphases (1 mM, self-buffered pH) and acidified water (pH 3.0) at the surface pressure 20 mN/m except for the case of Pb^{2+} : radiation, p polarization; incidence angle, 30° ; temperature, 22°C .

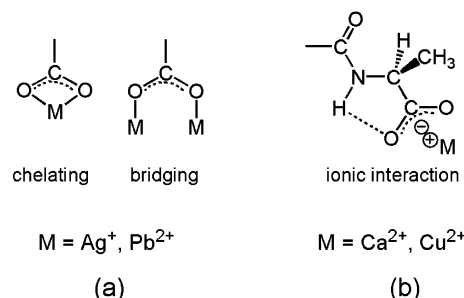


Figure 5. Schematic representation of metal coordination types and intramolecular hydrogen bond depending on metal ion.

of three-dimensional aggregates under these experimental conditions,³¹ i.e., crystallization at the air–water interface, whereas Ca^{2+} and Cu^{2+} ions give rise to the expansion of the film-forming molecules. The corresponding IRRAS spectra in Figure 4 can be classified into two categories from the profiles of the absorption bands.

In the case of Ag^+ , a strong band at 1512 cm^{-1} and a very weak peak at 1402 cm^{-1} are attributed to the asymmetric and symmetric carboxylate stretching vibrations [$\nu_a(\text{COO})$ and $\nu_s(\text{COO})$], respectively. The frequency separation between $\nu_a(\text{COO})$ and $\nu_s(\text{COO})$ is usually used as a diagnostic tool to gain an insight into the respective coordination types.³² A separation of 110 cm^{-1} between them suggests that a chelating or bridging bidentate coordination is formed between silver and carboxylate with a preference of covalent interaction, which is consistent with the favorable geometry of carboxylate to bind symmetrically to silver surface in the *n*-hexadecanoic acid monolayer.³³ The probable coordination types are schematically shown in Figure 5a. The amide A and amide I bands take a small shift to lower frequencies, suggesting that the intermolecular hydrogen-bonding interaction is slightly increased by the metal coordination. Compared with the monolayer on pure water, the $\nu_a(\text{CH}_2)$, $\nu_s(\text{CH}_2)$, and $\delta(\text{CH}_2)$ band frequencies remain unchanged, which suggests that both chain conformation and chain packing (triclinic subcell structure) are maintained. An obvious increase in band intensity also reflects formation of the three-dimensional structure.

In the case of Pb^{2+} , most of the bands are apparently doublets. The doublet features of these bands are distinguished when the spectra are collected at a resolution of 4 cm^{-1} (see part c of

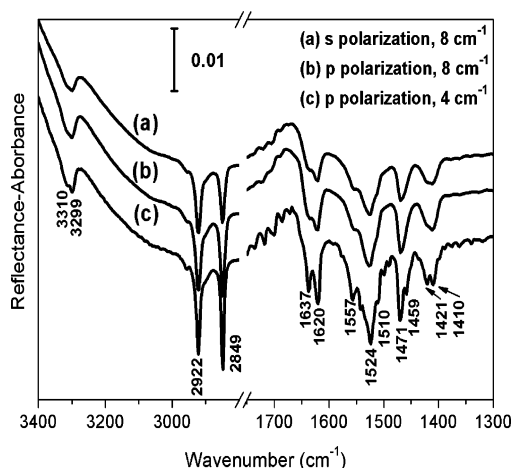


Figure 6. IRRAS spectra of the monolayers of *N*-octadecanoyl-L-alanine on Pb^{2+} -containing subphase at the incidence angle 30° : (a) s polarization, spectral resolution 8 cm^{-1} ; (b) p polarization, spectral resolution 8 cm^{-1} ; (c) p polarization, spectral resolution 4 cm^{-1} .

Figure 6). The two bands at 3310 and 3300 cm^{-1} are assigned to the amide A band, and the two bands at 1639 and 1625 cm^{-1} are due to the amide I band. It is clear that the intermolecular hydrogen-bonding interaction is obviously enhanced in the presence of Pb^{2+} . The enhanced intermolecular hydrogen-bonding interaction gives rise to an increase in amide II band frequency because this band takes an opposite change in frequency to amide A band, so the band at 1559 cm^{-1} is attributed to the amide II band. The broad band containing more than one component with a negative maximum at 1527 cm^{-1} is owing to the $\nu_a(\text{COO})$ vibration, and the doublet band at 1423 and 1410 cm^{-1} is assigned to a preference of $\nu_s(\text{COO})$ vibrations mixed with $\delta(\text{C}_\alpha\text{H}_2)$ modes.³⁴ The two types of metal coordination were reported for lead carboxylate in the literature,^{35,36} chelating bidentate coordination in the LB film of lead stearate [$\nu_a(\text{COO})$ at 1510 cm^{-1} and $\nu_s(\text{COO})$ at 1421 cm^{-1}]³⁵ and bridging bidentate coordination in the LB film of lead salt of poly(maleic acid) with octadecanol ester [$\nu_a(\text{COO})$ at 1540 cm^{-1} and $\nu_s(\text{COO})$ at 1400 cm^{-1}].³⁶ These spectral features in our case suggest that the two types of metal coordination with a preference of covalent bond constituent may be coexistent in the same system (see Figure 3a), which is consistent with the appearance of the doublet amide A and amide I bands.

The $\nu_a(\text{CH}_2)$ and $\nu_s(\text{CH}_2)$ vibrations are known to be sensitive to the conformational order of alkyl chains.²⁵ Lower wavenumbers are characteristic of highly ordered conformers with preferential all-trans chains, whereas the number of gauche conformers increases with wavenumbers and width of the band. The $\nu_a(\text{CH}_2)$ and $\nu_s(\text{CH}_2)$ frequencies in the case of Pb^{2+} take an upshift and downshift, respectively, as compared with those (2919 and 2851 cm^{-1}) in the case of pure water. This uncommon case is suggested to result from the overlap of the two $\nu_a(\text{CH}_2)$ and $\nu_s(\text{CH}_2)$ bands with different intensities, where some of the alkyl chains are composed of ordered all-trans conformers, and the others are populated with disordered gauche conformers. It is well-known that the electric vector of s polarization, E_s , is always parallel to the water surface. When the transition dipole moment of a functional group is parallel to E_s , the band intensity will be maximal. When the transition dipole moment is perpendicular to E_s , the band intensity will be undoubtedly minimal. The electric vector of p polarization is parallel to the plane of incidence direction and film normal. At the incidence angle 30° , a partial electric vector is perpendicular to the water surface in the case of p polarization. Parts a and b of Figure 6

compare the difference in intensity of the $\nu_a(\text{CH}_2)$ and $\nu_s(\text{CH}_2)$ bands for s and p polarization. The $\nu_s(\text{CH}_2)$ band intensity here is stronger than the $\nu_a(\text{CH}_2)$ one for p polarization, and it is reversed for s polarization. The spectral features suggest that the C—C—C planes of the alkyl chains are preferentially oriented perpendicular to the water surface.

However, completely different cases are encountered in the presence of Ca^{2+} and Cu^{2+} . The $\nu_a(\text{CH}_2)$ and $\nu_s(\text{CH}_2)$ bands appear at 2922 and 2853 cm^{-1} , respectively, indicative of disordered chain conformations. The bands in the region 1600 – 1500 cm^{-1} due to the $\nu_a(\text{COO})$ mode are very weak and broad. Such a weak feature has been attributed to the ionic interaction between metal ions and carboxylate groups.^{8,13} The amide A bands are substantially weakened and broadened around that region. These spectral changes imply that intramolecular hydrogen bonds may be formed between the amide and carboxylate groups. The IR bands of this kind of hydrogen bond are sometimes extremely broad, and the stronger the intramolecular hydrogen bond, the lower the intensity is.³⁷ It is likely that an intramolecular hydrogen bond is formed via a five-membered ring structure containing a chiral carbon atom between the H atom in N—H bond of the amide group and the O atom in C=O bond of the carboxylate group (see Figure 5b). The formation of the intramolecular hydrogen bond is further confirmed by the phase behavior of the thermotropic liquid crystal of the corresponding LB films with more than one phase process with the first transition temperature around 60 – 70°C similar to the phase temperature of stearic acid LB film.³¹ Clearly, the hydrogen bond in the monolayer undergoes a change in type and strength depending on metal ion in the subphase.

Conclusions

The NH stretching bands are for the first time observed using IRRAS technique from the monolayers of *N*-octadecanoyl-L-alanine at the air–water interface. The position and shape of the bands are related to type and strength of hydrogen bond. In the presence of Ag^+ and Pb^{2+} in the subphase, the covalent interaction between metals and carboxylate groups is favorable in the form of chelating and/or bridging bidentate coordination, and the intermolecular hydrogen-bonding interaction between the adjacent molecules through amide groups is increased in comparison with that in the case of pure water. In the presence of Ca^{2+} and Cu^{2+} , the ionic interaction between metal ions and carboxylate groups is preferred, and intramolecular hydrogen bond is developed at the expense of the original intermolecular hydrogen bond. The hydrogen bond in the monolayers at the air–water interface undergoes an obvious change in type and strength depending on metal ion in the subphase.

Acknowledgment. This work was financially supported by the Natural Science Foundation of China (Grant No. 20303008 and 20273029), Ministry of Education, and Nanjing University.

References and Notes

- (1) Maggiora, G. M.; Mao, B.; Chou, K. *New Developments in Molecular Chirality*; Mezey, G. P., Ed.; Kluwer Academic Publishers: Dordrecht, The Netherlands, 1991.
- (2) Nandi, N.; Vollhardt, D. *Chem. Rev.* **2003**, *103*, 4033.
- (3) Möhwald, H. *Annu. Rev. Phys. Chem.* **1990**, *41*, 441.
- (4) Knobler, C. M. *Adv. Chem. Phys.* **1990**, *77*, 397.
- (5) Kuzmenko, I.; Rapaport, H.; Kjaer, K.; Als-Nielsen, J.; Weissbuch, I.; Lahav, M.; Leiserowitz, L. *Chem. Rev.* **2001**, *101*, 1659.
- (6) Mendelsohn, R.; Brauner, J. W.; Gericke, A. *Annu. Rev. Phys. Chem.* **1995**, *46*, 305.
- (7) Gericke, A.; Hühnerfuss, H. *Langmuir* **1994**, *10*, 3782.
- (8) Hühnerfuss, H.; Neumann, V.; Stine, K. J. *Langmuir* **1996**, *12*, 2561.

- (9) Hoffmann, F.; Hühnerfuss, H.; Stine, K. *J. Langmuir* **1998**, *14*, 4525.
- (10) Overs, M.; Hoffmann, F.; Schäfer, H. J.; Hühnerfuss, H. *Langmuir* **2000**, *16*, 6995.
- (11) Grandbolis, M.; Desbat, B.; Blaudez, D.; Salesse, C. *Langmuir* **1999**, *15*, 6594.
- (12) Brauner, J. W.; Flash, C. R.; Xu, Z.; Bi, X.; Lewis, R. N. A. H.; McElhaney, R. N.; Gericke, A.; Mendelsohn, R. *J. Phys. Chem. B* **2003**, *107*, 7202.
- (13) Ren, Y.; Iimura, K.-i.; Kato, T. *Langmuir* **2001**, *17*, 2688.
- (14) Ren, Y.; Hossain, M. M.; Iimura, K.-i.; Kato, T. *J. Phys. Chem. B* **2001**, *105*, 7723.
- (15) Weck, M.; Fink, R.; Ringsdorf, H. *Langmuir* **1997**, *13*, 3515.
- (16) Huo, Q.; Dziri, L.; Desbat, B.; Russell, K. C.; Leblanc, R. M. *J. Phys. Chem. B* **1999**, *103*, 2929.
- (17) Flash, C. R.; Gericke, A.; Mendelsohn, R. *J. Phys. Chem. B* **1997**, *101*, 58.
- (18) Flash, C. R.; Gericke, A.; Keough, K. M. W.; Mendelsohn, R. *Biochim. Biophys. Acta* **1999**, *1416*, 11.
- (19) Lavoie, H.; Desbat, B.; Vaknin, D.; Salesse, C. *Biochemistry* **2002**, *41*, 13424.
- (20) Dluhy, R. A.; Cornell, D. G. *J. Phys. Chem.* **1985**, *89*, 3195.
- (21) Dluhy, R. A. *J. Phys. Chem.* **1986**, *90*, 1373.
- (22) Mitchell, M. L.; Dluhy, R. A. *J. Am. Chem. Soc.* **1988**, *110*, 712.
- (23) Miao, W.; Du, X.; Liang, Y. *J. Phys. Chem. B* **2003**, *107*, 13636.
- (24) Du, X.; Shi, B.; Liang, Y. *Langmuir* **1998**, *14*, 3631.
- (25) Snyder, R. G.; Hsu, S. L.; Krimm, S. *Spectrochim. Acta Part A* **1978**, *34*, 395.
- (26) Holland, R. F.; Nielsen, J. R. *J. Mol. Spectrosc.* **1962**, *9*, 436.
- (27) Dote, J. L.; Mowery, R. L. *J. Phys. Chem.* **1988**, *92*, 1571.
- (28) Peng, X.; Lu, R.; Zhao, Y.; Qu, L.; Chen, H.; Li, T. *J. Phys. Chem.* **1994**, *98*, 7052.
- (29) Clegg, R. S.; Hutchison, J. E. *Langmuir* **1996**, *12*, 5239.
- (30) Miao, W.; Du, X.; Liang, Y. *Langmuir* **2003**, *19*, 5389.
- (31) Du, X.; Liang, Y. *J. Phys. Chem. B* **2000**, *104*, 10047.
- (32) Nakamoto, K. *Infrared and Raman Spectra of Inorganic and Coordination Compounds*; John Wiley & Sons: New York, 1986.
- (33) Tao, Y.-T.; Lin, W.-L.; Hietpas, G. D.; Allara, D. L. *J. Phys. Chem. B* **1997**, *101*, 9732.
- (34) Du, X.; Liang, Y. *J. Phys. Chem. B* **2001**, *105*, 6092.
- (35) Peng, X.; Guan, S.; Chai, X.; Jiang, Y.; Li, T. *J. Phys. Chem.* **1992**, *96*, 6, 3170.
- (36) Li, L. S.; Qu, L.; Wang, L.; Lu, R.; Peng, X.; Zhao, Y.; Li, T. *J. Langmuir* **1997**, *13*, 6183.
- (37) Lin-Vien, D.; Colthup, N. B.; Fateley, W. G.; Grasselli, J. G. *The Handbook of Infrared and Raman Characteristic Frequencies of Organic Molecules*; Academic Press: San Diego, 1991.